Heliyon 10 (2024) e37019

Contents lists available at ScienceDirect

Heliyon

journal homepage: www.cell.com/heliyon

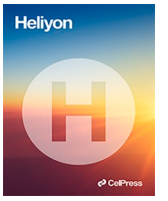

Research article

Astragaloside IV ameliorates pressure overload-induced heart failure by enhancing angiogenesis through HSF1/VEGF pathway

Peizhao Du [a,1], Linghao Xu [b,c,1], Yuanqi Wang [c,1], Tiantian Jiao [c], Jing Cheng [c], Chunsheng Zhang [d], Md Sakibur Rahman Tapu [c], Jian Dai [a,**], Jiming Li [c,*]

[a] Department of Cardiology, Baoshan District Hospital of Integrated Traditional Chinese and Western Medicine of Shanghai, Shanghai University of Traditional Chinese Medicine, Shanghai, 201999, China
[b] Department of Endocrinology and Metabolism, The Affiliated Hospital of Southwest Medical University, Luzhou, Sichuan 646000, China
[c] Department of Cardiology, Shanghai East Hospital, School of Medicine, Tongji University, Shanghai, 200092, China
[d] Department of Cardiology, East Hospital of Clinical Medical College, Nanjing Medical University, Nanjing, 211166, China

ARTICLE INFO

Keywords:
Astragaloside IV
Heat shock transcription factor 1
Vascular endothelial growth factor
Angiogenesis
Heart failure

ABSTRACT

Astragaloside IV(AS-IV), the main active ingredient of Astragalus, has been used as a treatment for heart failure with favorable effects, but its molecular mechanism has not been fully elucidated. Network pharmacological analysis and molecular docking revealed that Heat shock transcription factor 1 (HSF1) is a potential target of AS-IV. We designed cellular and animal experiments to investigate the role and intrinsic molecular mechanisms of AS-IV in ameliorating pressure overload-induced heart failure. In cellular experiments, Myocardial microvascular endothelial cells (MMVECs) were cultured in isolation and stimulated by adding high and low concentrations of AS-IV, and a cell model with down-regulation of HSF1 expression was constructed by using siRNA technology. Changes in the expression of key molecules of HSF1/VEGF signaling pathway and differences in tube-forming ability were detected in different groups of cells using PCR, WB and tube-forming assay. In animal experiments, TAC technology was applied to establish a pressure overload-induced heart failure model in C57 mice, postoperative mice were ingested AS-IV by gavage, and adenoviral transfection technology was applied to construct a mouse model with down-regulation of HSF1 expression.Small animal ultrasound for cardiac function assessment, MASSON staining, CD31 immunohistochemistry, and Western blotting (WB) were performed on the mice. The results showed that AS-IV could promote the expression of key molecules of HSF1/VEGF signaling pathway, enhance the tube-forming ability of MMVECs, increase the density of myocardial capillaries, reduce myocardial fibrosis, and improve the cardiac function of mice with TAC.AS-IV could modulate the HSF1/VEGF signaling pathway to promote the angiogenesis and improve the pressure overload-induced heart failure.

* Corresponding author.
** Corresponding author.
E-mail addresses: dj0056@shutcm.edu.cn (J. Dai), ljm13303818674@126.com (J. Li).
[1] These authors contributed equally to this work.

https://doi.org/10.1016/j.heliyon.2024.e37019
Received 27 February 2024; Received in revised form 24 August 2024; Accepted 26 August 2024
Available online 1 September 2024

1. Introduction

Heart failure is a multifaceted clinical syndrome resulting from abnormal structure and function in the heart due to various causes, leading to impaired ventricular systolic or diastolic function [1]. As the ultimate stage in diverse heart diseases, heart failure is prone to recurrence, challenging to remedy, and exhibits a grim prognosis. It has emerged as a pivotal factor jeopardizing human health, intensifying societal and familial economic burdens [1]. Current guidelines advocate pharmacological interventions for heart failure, primarily encompassing angiotensin-converting enzyme inhibitors (ACEI), diuretics, angiotensin receptor blockers (ARB), β-receptor blockers, and mineralcorticoid receptor antagonist(MRA) [2,3]. While these medications ameliorated symptoms and notably enhanced survival in heart failure patients, they did not reduce overall mortality [4]. Furthermore, common challenges in the present pharmacological management of heart failure include adverse effects like electrolyte imbalances, blood pressure fluctuations, and drug resistance [5]. Confronted with the dilemma of heart failure treatment, innovative therapeutic approaches are urgently needed.

Chinese medicine boasts a rich history in heart failure treatment. Astragaloside IV (AS-IV), the primary active compound in Astragalus membranaceus, a traditional Chinese remedy for heart failure, is characterized as a distinctive saponin with a molecular formula of $C_{41}H_{68}O_{14}$ and a molecular weight of 784.97(Fig. 1A) [6].Numerous lines of evidence substantiate the effectiveness and safety of AS-IV in both in vivo and in vitro heart failure models [7,8]. Studies have revealed that AS-IV's mechanism in heart failure treatment encompasses various facets of heart failure pathophysiology. These include protection against myocardial ischemia [9,10], modulation of sarcoplasmic reticulum calcium pumps [11,12], improvement of myocardial energy metabolism [13], inhibition of myocardial hypertrophy [14,15], anti-inflammation [16], and inhibition of oxidative stress [17,18], among others. Nevertheless, further elucidation is required concerning the direct targets and mechanisms of action.

Heat shock transcription factor 1 (HSF1) serves as a transcription factor for various heat shock proteins (HSPs), exhibiting high conservation across species, extensive structural and functional homology, and ubiquitous presence in eukaryotic cells. It is crucial for the organism's response to heat shock [19]. In our prior studies, we identified that HSF1 induces the expression of heat shock proteins, including HSP70 and HSP90, and upregulates the expression of HIF-1 and VEGF. This cascade, in turn, fosters angiogenesis, enhances myocardial blood supply, improves the heart's ejection capacity, and ultimately retards the progression of heart failure. HSF1 assumes a pivotal protective role in the pathological process of heart failure [20].

By utilizing network pharmacology analysis and molecular docking techniques, we identified the HSF1/VEGF pathway as a potential target for AS-IV's action. Subsequently, we formulated a hypothesis positing that AS-IV may mitigate heart failure through modulation of the HSF1/VEGF signaling pathway.

2. Materials and methods

2.1. Network pharmacologic analysis

AS-IV's chemical structure was obtained from PubChem database [21]. Swisstarget prediction database [22] was used to predict the targets after inputting the SDF file of AS-IV. Gene Cards database was used to find related disease targets for heart failure [23]. The overlapped targets were entered into the STRING database [24] and the essential proteins underwent topological analysis via Cytoscape 3.10.1 [25]. The overlapped targets integrated into the Metascape database [26] to conduct Gene Ontology (GO) and Kyoto Encyclopedia of Genes and Genomes (KEGG) pathway enrichment analyses. Heatmap was generated through bioinformatics platform for visualization [27]. The website are listed in the supplementary information.

2.2. Molecular docking

The 3D structures of HSF1 were obtained from the PDB website(https://doi.org/10.2210/pdb5hdn/pdb). The molecular structure of AS-IV and HSF1 were optimized via PyMOL software (version 2.5.7) [28]. The active site was encompassed within a single gridbox, centrally positioned at x = 15.507, y = −0.991, z = 27.283 Å, and exhibiting dimensions of 98 Å, 90 Å, and 122 Å along the corresponding edges. The process of molecular docking was carried out utilizing AutoDock Tools software (version 1.5.7) [29].

2.3. Cell culture and treatment

Primary myocardial microvascular endothelial cells (MMVECs) were isolated, cultured, and characterized following our previously established article [30]. Specifically, tissue explants were utilized for the culture of MMVECs. Male C57/BL6 mice, aged 8–12 weeks, were selected and euthanized via anesthesia using 10 % chloral hydrate at a dosage of 0.3 mL/100 g. Following immersion in 75 % ethanol for sterilization, the hearts were excised under sterile conditions and placed in sterile culture dishes. The atria, visible connective tissue, and valvular tissue were removed, and the remaining cardiac tissue was finely minced into approximately 2 mm^3 pieces. Following the addition of 1 mL of fetal bovine serum, the minced tissue fragments were evenly distributed into two culture flasks. The cultures were then incubated at 37 °C with 5 % CO_2 and saturated humidity for 4 h. Subsequently, 2 mL of DMEM supplemented with 20 % fetal bovine serum was added. The culture medium was replaced after 24 h. After approximately 72 h of incubation, the tissue fragments were removed once substantial cell growth was observed surrounding the tissues. Subsequently, microscopy was employed to investigate the morphological characteristics of MMVECs as they approached a sub-confluent state, nearly covering the bottom of the culture flasks. The purity of the MMVECs was evaluated by staining with an anti-VIII factor antibody (Abcam, USA, 1:200) following standard protocol procedures. MMVECs at passages 4 to 8 were cultured in DMEM/F12 (ShanghaiBasalmedia, China)

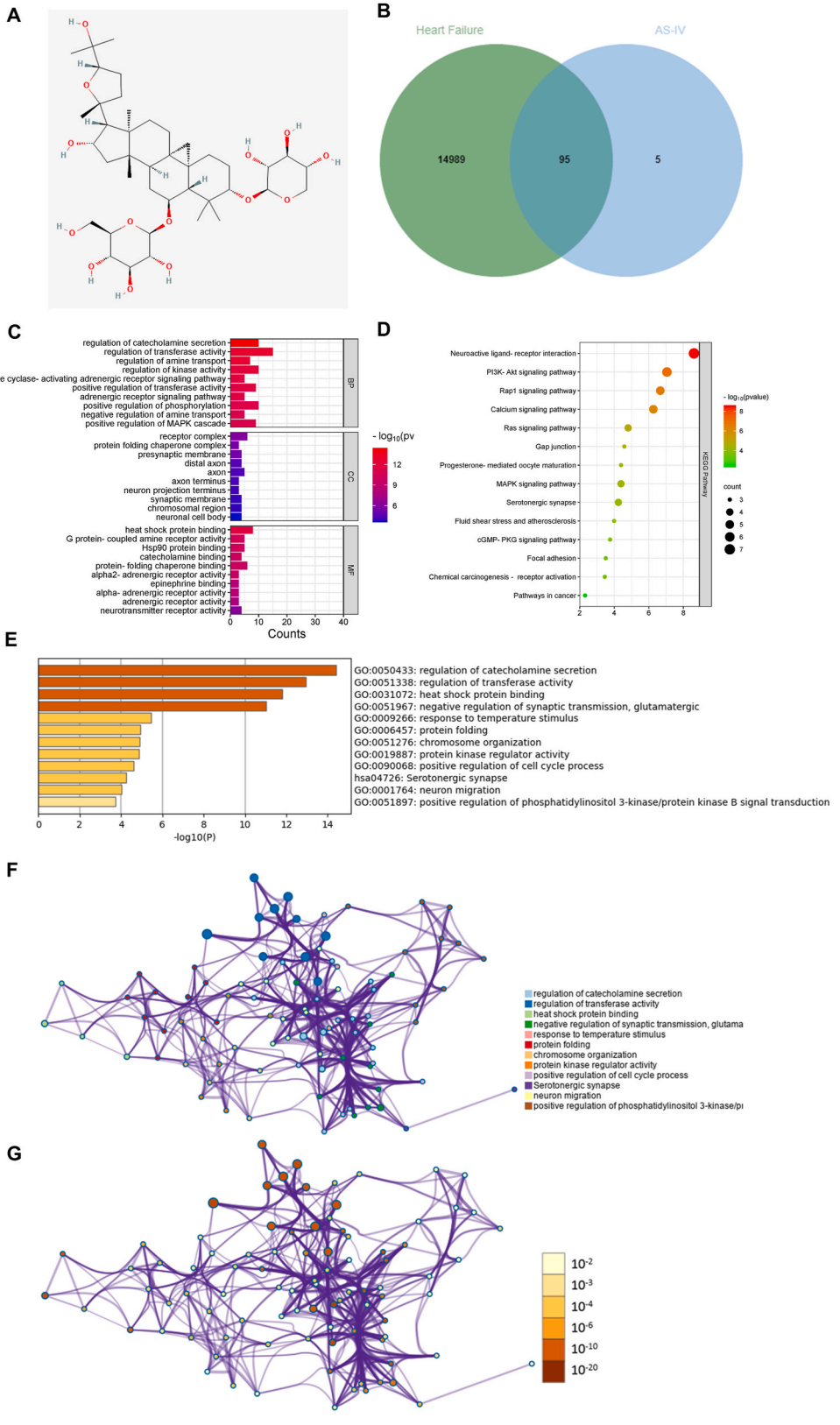

(caption on next page)

Fig. 1. Network pharmacologic analysis for AS-IV (A)2D structure of AS-IV (B)Common targets of AS-IV and heart failure (C)GO enrichment analysis($p < 0.05$) (D) KEGG pathway analysis($p < 0.05$) (E) Heatmap representation of enriched terms through Metascape with coloration based on p-values ($p < 0.05$) (F) Network visualization of enriched clusters based on identity through Metascape. ($p < 0.05$) (G) Differentially Expressed Genes (DEGs) enriched clusters arranged by significance via Metascape ($p < 0.05$).

medium containing 10 % fetal bovine serum (FBS) (Gibco,America), 1 % penicillin with streptomycin (NCM Biotech,Suzhou,China) in 5 % CO_2 at 37 °C. The medium was replaced every 2–3 d. Various concentrations of AS-IV (10uM, 20uM) were used to treat the cells.

2.4. RNA interference

Primary MMVECs were seeded in 6-well plates the day prior to transfection. RNAiMAX (Invitrogen, Carlsbad, CA) was utilized to transfect 50 nM of HSF1 siRNA (Santa Cruz Biotechnology, Santa Cruz, CA, USA) into the cells with OPTI-MEM Medium (Invitrogen) for 48 h. Control siRNA containing a scrambled sequence (Santa Cruz) was utilized as a negative control.

2.5. RT-PCR analysis

Total RNA was extracted from each experimental group using TRIZOL reagent (Life Technologies,America) following the manufacturer's instructions. Subsequently, RNA was purified using the RNeasy Minikit (Qiagen, Valencia, CA) and treated with RNase-free DNase (Qiagen, CA) in order to remove any genomic DNA contamination. The condition for conducting quantitative reverse-transcriptase PCR (RT-PCR) was as follows 30 s at 95 °C, 40 cycles of 5 s at 95 °C,34 s at 60 °C, and 30 s at 72 °C. The PCR utilized specific primer pairs as follows:

HSF1 sense: 5′- GTTACCAGGGCTGCCTTCTC -3′, antisense: 5′- TTCTCAGCCTTGACTGTGCC -3';

GAPDH sense: 5′- GCCATCACTGCCACTCAGAA-3′, antisense: 5′- GGCATGTCAGATCCACAACG-3.

Data analysis was carried out using the ABI PCR system 7500(Applied Biosystems, America). Using the $2^{-\triangle\triangle Ct}$ method to analyze the relative changes in mRNA with GAPDH as the internal reference gene.

2.6. Tube formation

According to our previously established article [30], Dissolved Matrigel (Corning Inc.) was added to cover the bottom of 96-well plates (50μL/well) on ice followed by solidification through incubation at 37 °C for 30 min. Subsequently, MMVECs (5×10^3/well) resuspended in endothelial cell medium were seeded in the 96-well plates. Five fields were counted for each well after 8 h and the length of the tube was quantified by Image J(NIH, Bethesda, USA).

2.7. Animals and reagents

Male adult wild-type (WT) mice (C57BL/6J, 8 weeks of age) were procured from the Shanghai Animal Administration Center (Shanghai, China). The weight of the mice varied between 25 and 30 g. Mice were kept in standard conditions, which included a 12-h cycle of light and darkness, and they had unrestricted access to water and standard mouse food provided in the laboratory. AS-IV was purchased from Selleck.

2.8. Establishment of TAC and grouping

The Transverse Aortic Constriction (TAC) model established in our previous study was used to induce pressure overload-induced hypertrophy and heart failure [31]. In summary, the mice were anesthetized using isoflurane and positioned supine. A thoracotomy was performed, and the transverse aortic constriction was carefully isolated from the surrounding tissues and muscles at the level of the aortic arch. A 6-0 nylon suture was then placed around the aorta using a blunt 27-gauge needle, which was subsequently removed following the ligation. The SHAM group went through all operation procedures excluding the ligation. Mice were administered AS-IV (40 mg/kg/d) by gavage post-surgery. Simultaneously constructing a model with downregulated HSF1 expression by applying adenovirus transfection technology, then assigned the mice into SHAM group, TAC group, TAC + AS-IV group and TAC + AS-IV + HSF1 Ad group, which were observed at 8 weeks post-surgery.

2.9. Constructs and transfection of adenoviral vectors

To construct the adenovirus, the pADV-U6-shRNA-CMV-EGFP vector was designed by OBiO Technology(Shanghai China). Specifically, shRNA targets were designed based on the transcript of the Mouse HSF1 gene, and primers were synthesized accordingly. The single-stranded primers were annealed to form double-stranded oligonucleotide sequences, which were then ligated into a double enzyme-linearized RNA interference vector, replacing the original ccdB toxicity gene. Transformants were screened using colony PCR, and positive clones were subjected to sequencing for validation. Correct clones were verified through sequencing, followed by high-purity plasmid extraction. The sketch map of vector and gene sequence can be found in supplement PDF. The viral titer exceeds 1 × 10^12 viral genomes per milliliter, and an aliquot of 200 μL is administered via tail vein injection to each mouse immediately after TAC

and 4 weeks after TAC.

2.10. Measurement of echocardiography

Cardiac geometry and function were assessed via transthoracic echocardiography utilizing Vevo2000 (VisualSonics, Canada). Mice were anesthetized with isoflurane (5 % isoflurane and O_2 mixture) using a ventilation apparatus, and 2D echocardiographic measurements were acquired. All data represent the means derived from a minimum of 5 cardiac cycles in M-mode echocardiography for each mouse, including left ventricular internal dimension systole (LVIDs) and left ventricular internal dimension diastole (LVIDd), along with the ejection fraction (EF) and fractional shortening (FS).

2.11. Test of histopathology

After sacrificing the mice and immediately harvesting their hearts, heart weight was measured. To perform histological examination, heart tissues were preserved in 4 % neutral formaldehyde at 25 °C for more than 24 h. The samples were then encased in paraffin and cut into 4 μm thick consecutive sections along the short axis at the level of the papillary muscle, and subsequently stained with Masson trichrome in order to examine fibrosis in cardiomyocytes. Quantification of the fibrotic region in cardiomyocytes was performed on three slices from each heart, and the mean of five randomly selected high power fields was calculated for each section.

2.12. Evaluation of microvessel density

Immunohistochemical analysis was employed to assess angiogenesis following treatment, since CD31 is expressed in newly developed vascular endothelial cells. According to the method described earlier [32], the positive signal of CD31 in the newly formed vascular was visualized through orange-yellow staining. Microvessel enumeration was conducted using a microscope at a 400-fold magnification. The quantification of angiogenesis was measured utilizing Image J (NIH, Bethesda, USA).

2.13. Western blotting analysis

Hearts were rapidly frozen in liquid nitrogen and stored at −80 °C. Meanwhile, cells were washed twice with phosphate-buffered saline (PBS) before proceeding with protein extraction. Heart tissues were homogenized and sonicated in RIPA buffer (Shanghai Epizyme, China) supplemented with a protease inhibitor cocktail (Shanghai Epizyme, China) while the same buffer was added to cells and then dissociated on ice for 30 min. Liquid supernatant was meticulously collected after centrifugation. Protein concentration was measured using the BCA reagent kit (Shanghai Epizyme, China), and appropriate loading buffer was added. To mitigate the potential cross-reactivity among distinct antibodies and optimize image quality by accounting for varying exposure durations, we implemented a method involving uniform sample loading and individualized incubation exposures. A total of 30 μg of protein per lane was loaded onto an SDS-PAGE gel and subsequently transferred to a PVDF membrane (Merck, Germany). At 4 °C, the PVDF membrane was subjected to overnight incubation with primary antibody purchased from Abcam (Cambridge, MA, USA) including HSF1, HSP70, HIF-1α, VEGF and β-actin at 4 °C overnight. Then the membrane was washed with Tris buffered saline with tween (TBST) and incubated with horseradish peroxidase (HRP)-coupled secondary antibody (Biyuntian, China, 1:2000) for 60 min at 25 °C. The luminous signal was observed with Tanon 5200 multifunctional image analysis system (Tanon Technology, Shanghai, China). The average gray values of the bands were analyzed utilizing Image J (NIH, Bethesda, USA) with β-actin serving as the internal reference protein.

2.14. Statistical analysis

All data are expressed with mean ± Standard Deviation (SD). Statistical significance were conducted using *t*-test between two groups or one-way ANOVA followed by Tukey's post hoc analysis between multiple comparisons. Statistical analysis was conducted utilizing GraphPad Prism 8.0 software (GraphPad, San Diego, CA). A p value < 0.05 was regarded as statistically significant.

3. Results

3.1. HSF1 is a potential target for AS-IV in heart failure treatment

AS-IV's chemical structure was sourced from PubChem, and its targets were predicted using Swisstarget prediction after inputting the SDF file. Gene Cards identified disease targets related to heart failure, and overlapping targets were subjected to topological analysis using Cytoscape following analysis in the STRING database. A network pharmacology approach was utilized to predict the molecular targets of AS-IV. As shown, AS-IV had 100 targets, and heart failure had 15084 targets. The intersection of AS-IV and heart failure targets yielded 95 genes as potential targets for AS-IV in heart failure treatment(Fig. 1B).

The core genes were further screened for enrichment analysis. The average value of node connectivity (degree) was selected as the screening criterion, and a Hub network consisting of 20 core genes was extracted. These targets play a key role in the protein-protein interaction(PPI) networks and may be the main targets for disease treatment through drug intervention. These 20 targets were analyzed using GO enrichment for biological processes (BP), cellular components (CC) and molecular functions (MF). For BP, AS-IV intervention was mainly related to "regulation of catecholamine secretion" and "regulation of transferase activity". For CC, there

was significant enrichment of genes mainly related to “receptor complex” and “protein folding chaperone complex”. For MF, the targets were closely related to “heat shock protein binding” and “G protein-coupled amine receptor activity” (Fig. 1C). KEGG pathway enrichment analysis indicated that AS-IV-related genes were predominantly associated with “neuroactive ligand-receptor interactions” and the signaling pathways including “cGMP-PKG signaling pathway” and “PI3K-Akt signaling pathway”(Fig. 1D). Moreover, the analysis of functional enrichment with Metascape showed that core genes of AS-IV interventing heart failure were significantly enriched in “regulation of catecholamine secretion”, “regulation of transferase activity” and “heat shock protein binding”(Fig. 1E–G).

Under normal conditions, HSF1 exists as an inactive monomer in the cytoplasm, binding to specific HSPs. When exposed to stressors like thermal stimulation or hypoxia, proteins in the cytoplasm undergo damage and denaturation. HSPs bind to the damaged proteins, releasing HSF1 monomers. These monomers polymerize into transcriptionally active trimers. After phosphorylation modification, they translocate to the nucleus, binding to the heat shock element (HSE) in the promoter region of the HSP gene. This activation of transcription leads to the production of HSPs, enhancing cellular resistance to damage [19,33],Thus, HSF1 is closely related to the "protein folding chaperone complex" and "heat shock protein binding" pathways analyzed in our study [34]. Our previous research supports that the HSF1/VEGF signaling pathway promotes angiogenesis, improves myocardial blood supply, cardiac ejection capacity, and delays the progression of heart failure [20,35],HSF1 acts as the triggering molecule in this pathway. Hence, we hypothesize that

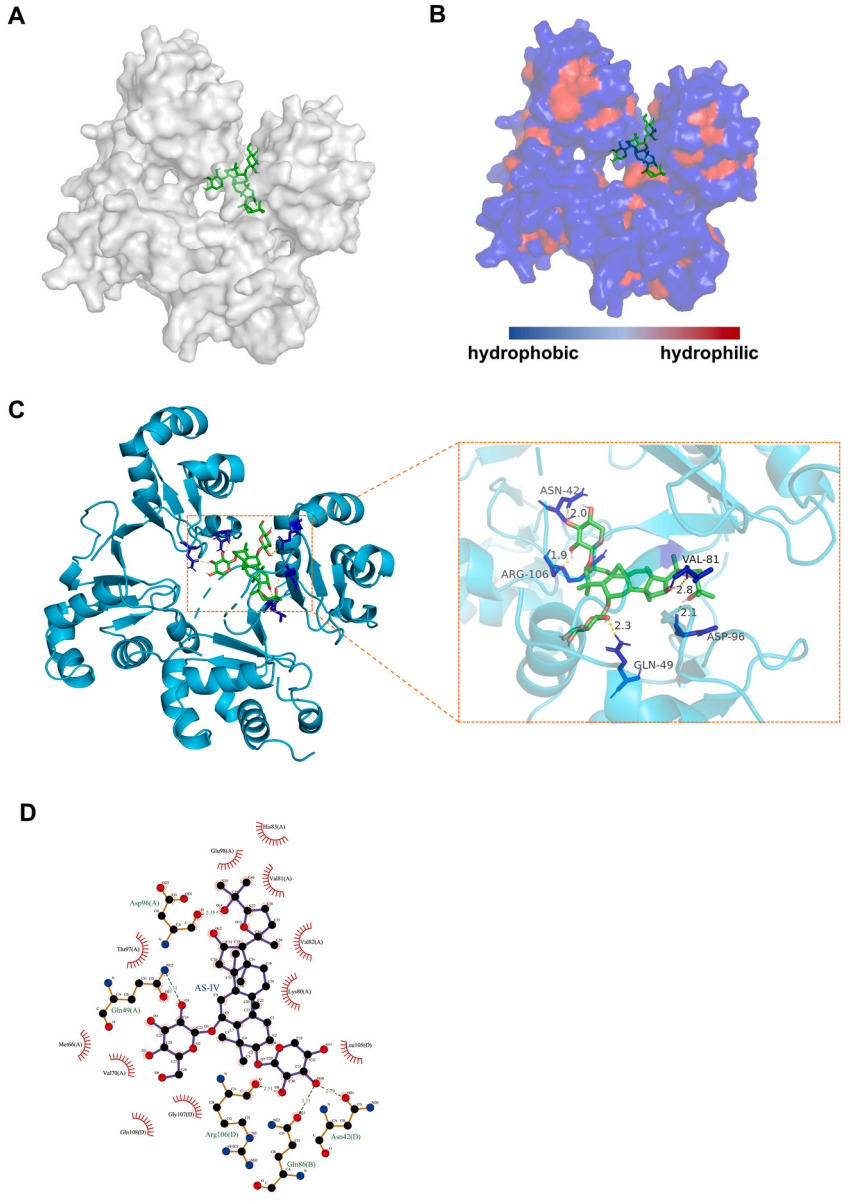

Fig. 2. Molecular docking for AS-IV and HSF1 (A) Representative images of autodocking for AS-IV and HSF1 (B)Hydrophilicity and hydrophobicity of surface of the protein–ligand complex (C) Interaction maps of the protein–ligand complex (D) Hydrogen bonds in binding site.

HSF1 may be a target for AS-IV in treating heart failure.

We analyzed AS-IV and HSF1 using molecular docking. Molecular docking is a well-established computer structure-based method that can predict ligand-target interactions at the molecular level and can help explore novel therapeutic applications for clinical drugs, natural compounds and synthesized chemicals [36]. The results indicated a well-matched binding pocket on the surface of AS-IV and HSF1 with an binding affinity of −6.36 kcal/mol(Fig. 2A). According to previous studies, docking ability is considered present when the binding affinity is lower than −1.2 kcal/mol, and it is generally considered good when the binding affinity is lower than −5 kcal/mol [37].In addition, the binding site is highly hydrophilic(Fig. 2B), and HSF1 residues Asn42, Arg106, Val81, Gln49 and Asp96 are involved in the formation of hydrogen bonds with the hydroxyl group of AS-IV(Fig. 2C–D), which is necessary for stable binding. In summary, HSF1 is a potential target of AS-IV in the treatment of heart failure.

3.2. *AS-IV promotes elevated expression of HSF1 and its downstream molecules in MMVECs, and inhibition of HSF1 expression blocks this effect*

MMVECs were cultured in isolation(Fig. 3A), and RT-PCR assay were performed after adding different concentrations of AS-IV and transfected with HSF1 siRNA. RT-PCR results revealed an increased HSF1 mRNA expression level in the AS-IV LD group compared to NC, with a further increase in the HSF1 expression level in the AS-IV HD group(Fig. 3B). In contrast, HSF1 mRNA expression decreased in the AS-IV HD + HSF1 siRNA group. Our supplementary data clearly shows significant differences expression of protein between the NC and HSF1 siRNA groups following HSF1 knockdown (Fig. S1). WB results indicated elevated expression levels of HSF1, HSP70, HIF-1α, and VEGF in the AS-IV LD group compared to the NC group, with further increases in the AS-IV HD group.The AS-IV HD + HSF1 siRNA group exhibited significantly lower expression of the mentioned four proteins compared to the AS-IV LD and AS-IV HD groups,

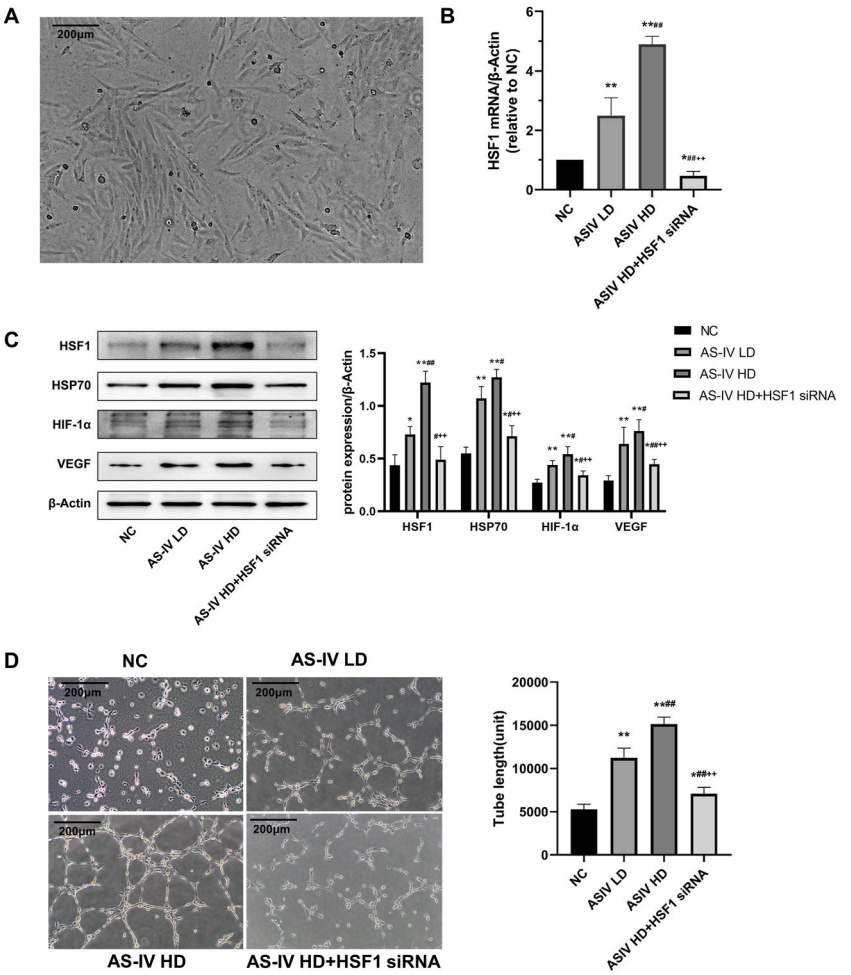

Fig. 3. AS-IV promotes angiogenesis of MMVECs through the HSF1/VEGF pathway (A) MMVECs (200 ×) (B) RT-PCR detection for HSF1 mRNA expression levels of MMVECs in each group (C)WB detection for HSF1, HSP70, HIF-1α, and VEGF expression levels of MMVECs in each group (D) Tube formation assay to test the tube-forming ability of MMVECs in each group and analysis of the results (200 ×) (n = 3.*$p < 0.05$ vs NC, **$p < 0.01$ vs NC, #$p < 0.05$ vs AS-IV LD, ##$p < 0.01$ vs AS-IV LD, + $p < 0.05$ vs AS-IV HD, ++ $p < 0.01$ vs AS-IV HD).

with the apparent lack of difference in the NC and AS-IV HD + HSF1 siRNA group attributed to AS-IV-induced upregulation of HSF1 expression.(Fig. 3C).

3.3. AS-IV enhances tube-forming ability of MMVECs, and inhibition of HSF1 expression blocks this effect

Experiments on tube formation demonstrated a notable elevation in tube length within the AS-IV LD group, further increased in the AS-IV HD group compared to the NC group. However, the length of tubes in the AS-IV HD + HSF1 siRNA group was significantly decreased compared to the AS-IV LD and AS-IV HD groups(Fig. 3D).

3.4. AS-IV improves cardiac function of mice with pressure overload-induced heart failure, and inhibition of HSF1 expression results in a significant reduction of this benefit

After interventions via ascending aortic narrowing, gavage administration, and adenoviral transfection, mice underwent ultrasonographic examination of the heart in the 8th week post-operation. Compared with the SHAM group, the TAC group exhibited a significant decrease in EF and FS values, widening of systolic and diastolic LVIDs, and an increase in cardiac body weight ratio, indicating successful heart failure model construction. Conversely, the group receiving AS-IV post-surgery demonstrated notable improvements in EF and FS values, reduction in systolic-diastolic LVID, and a decrease in cardiac body weight ratio compared to the TAC group, suggesting AS-IV's efficacy in enhancing cardiac ejection function and mitigating cardiac remodeling post-TAC. To explore the function of HSF1 in the TAC + AS-IV group, we employed adenovirus transfection to create a model where HSF1 expression was downregulated using shRNA targeting HSF1 via tail vein injection (Fig. S2). However, mice in the TAC + AS-IV + HSF1 Ad group, when compared with the TAC + AS-IV group, exhibited diminished EF and FS values, widened systolic-diastolic LVID, and increased heart weight ratio(Fig. 4A–B).

3.5. AS-IV reduces myocardial fibrosis and promotes myocardial capillary proliferation in pressure-overload heart failure mice, and inhibition of HSF1 expression reverses this effect

Cardiac sections from mice in every group were obtained and underwent MASSON staining as well as CD31 immunohistochemical staining of myocardial tissues. The degree of fibrosis and microvessel density were analyzed after capturing microscope images. The results revealed a significantly higher degree of myocardial fibrosis in the TAC group than in the SHAM group, accompanied by increased myocardial capillary density. The TAC + AS-IV group exhibited a reduced level of myocardial fibrosis compared to the TAC group, resulting in a decrease in myocardial capillary density. Nevertheless, in the TAC + AS-IV + HSF1 Ad group, there was an elevated level of myocardial fibrosis compared to the TAC + AS-IV group, accompanied by a simultaneous reduction in myocardial capillary density (Fig. 4C–D).

AS-IV promotes the expression of HSF1 and key molecules of its downstream pathway in the myocardium of pressure-overloaded heart failure mice, and inhibition of HSF1 expression blocks this effect.

Adenovirus successfully knocked down the expression of HSF1 gene and protein in mouse cardiac tissue (Fig. S2). Myocardial tissue proteins were extracted from each mouse group, and WB was used to assess the myocardial expression of HSF1, HSP70, HIF-1α, and VEGF. The results revealed elevated expression of these four molecules in the TAC group compared to SHAM. Moreover, in the TAC + AS-IV group, the expression of the four proteins was further increased compared to the TAC group.In contrast, the TAC + AS-IV + HSF1 Ad group exhibited a decrease in the expression of these four proteins compared to the TAC + AS-IV group. The protein expression levels in the TAC + AS-IV + HSF1 Ad group closely resembled those in the Sham group, suggesting that the upregulating effect of AS-IV on proteins was partially counteracted by HSF1 Ad. (Fig. 5).

4. Discussion

In this study, we discovered that AS-IV positively regulates the HSF1/VEGF signaling pathway, leading to an improvement in pressure overload-induced heart failure. This improvement is attributed to the promotion of angiogenesis and reduction in myocardial fibrosis through this pathway.

Network pharmacology analysis revealed significant enrichment of AS-IV targets intervening heart failure in "protein folding chaperone complex" and "heat shock protein binding". The results of molecular docking simulations suggested that AS-IV has the good capability to bind to HSF1. We postulated that AS-IV binds to HSF1, activating its downstream pathway for heart failure treatment. Subsequently, we devised cellular and animal experiments to validate this hypothesis.

In the cellular experiment part, we added different concentrations of AS-IV to MMVECs, and found that AS-IV can promote the elevated expression of HSF1 at the mRNA and protein levels, and its downstream key molecules, HSP70, HIF-1α, and VEGF protein expression levels were likewise elevated, and this effect demonstrated a positive correlation with the concentration of AS-IV within a specific range. Meanwhile, we found that the tube-forming ability of MMVEC was enhanced after the addition of AS-IV, which was correlated with the elevated expression level of VEGF. In contrast, after inhibition of HSF1 expression by siRNA technology, the role of AS-IV in promoting MMVEC tube formation was weakened, while no elevated expression of VEGF molecules was detected. Accordingly we demonstrated at the ex vivo level that AS-IV could modulate the HSF1/VEGF pathway to promote angiogenesis of MMVECs.

In the animal experiment part, our experimental results found that TAC 8W mice had increased cardiac body weight ratio, decreased cardiac EF and FS, and widened LVID, indicating that the heart failure model was constructed successfully. Tissue section

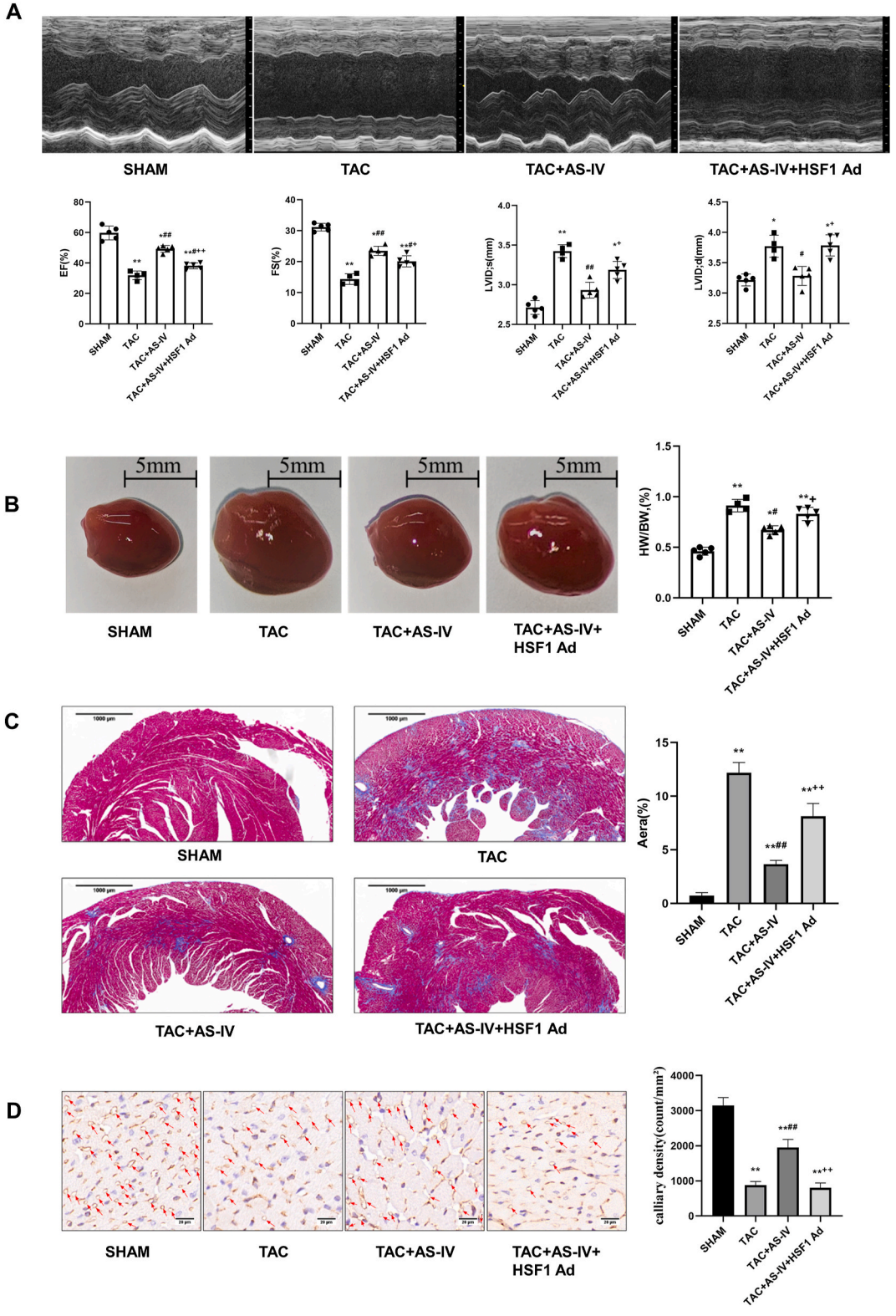

(caption on next page)

Fig. 4. Protective effects of AS-IV in pressure-overloaded mice (A)Ultrasonographic examination of the mice's hearts in each group and analysis of the results (B)Gross observation of the mice's hearts in each group and analysis of the results of heart weight ratio detection (C) MASSON-stained sections and analysis of the degree of myocardial fibrosis of mice's hearts in each group (D) Immunohistochemical staining of CD31 and analysis of myocardial capillary density in mice's hearts in each group (n = 4 in TAC group and n = 5 in other group.*$p < 0.05$ vs SHAM, **$p < 0.01$vsSHAM, #$p < 0.05$ vs TAC, ##$p < 0.01$ vs TAC, + $p < 0.05$ vs TAC + AS-IV, ++ $p < 0.01$ vs TAC + AS-IV).

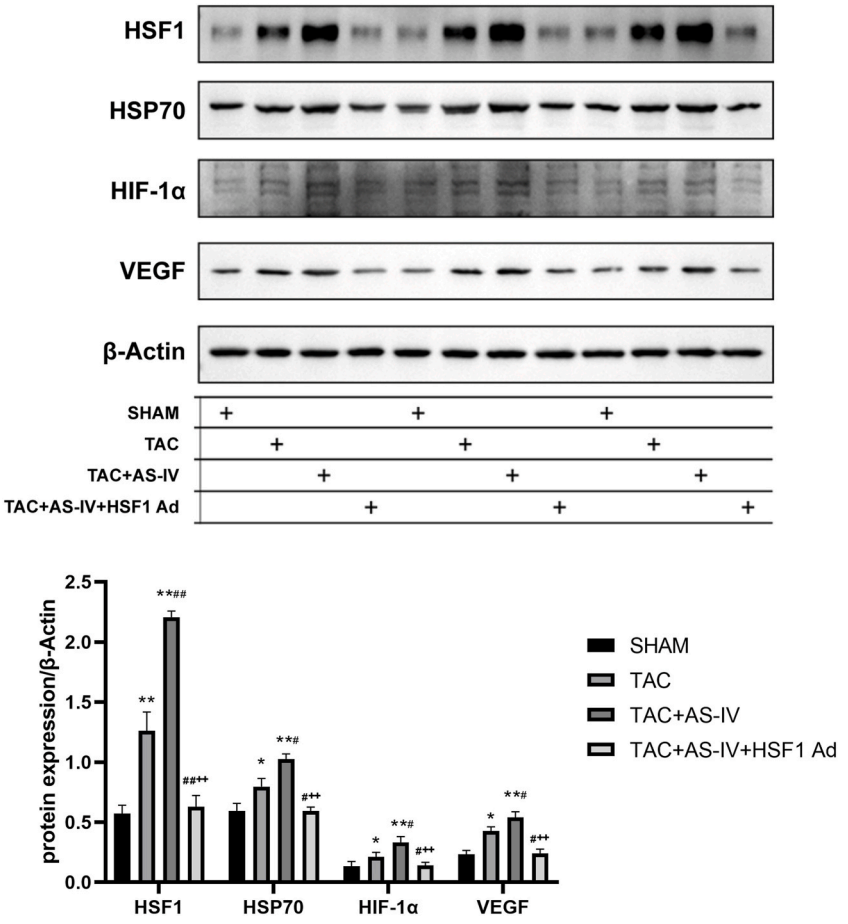

Fig. 5. Results of WB assays for HSF1, HSP70, HIF-1α, and VEGF of mice's myocardium in each group (n = 4 in TAC group and n = 5 in other group. *$p < 0.05$ vs SHAM, **$p < 0.01$vsSHAM, #$p < 0.05$ vs TAC, ##$p < 0.01$ vs TAC, + $p < 0.05$ vs TAC + AS-IV, ++ $p < 0.01$ vs TAC + AS-IV).

staining revealed increased cardiac fibrosis and decreased endothelial density of myocardial capillaries in TAC 8W mice, which was consistent with the pathological manifestations of heart failure. In contrast, when mice were given AS-IV by gavage feeding after TAC, the cardiac function of mice was significantly improved, myocardial fibrosis was reduced, and the density of myocardial capillary network was increased, suggesting that AS-IV could improve heart failure and was associated with angiogenesis. The WB results suggested that AS-IV promotes the elevated expression of HSF1, HSP70, HIF-1α, and VEGF, which preliminarily suggests that AS-IV can regulate the HSF1/VEGF signaling pathway. To further confirm the role of AS-IV through HSF1, we utilized adenoviral transfection to inhibit HSF1 expression in mice. Results showed that after HSF1 inhibition, the efficacy of AS-IV in improving cardiac function was diminished, the level of VEGF expression did not increase, and myocardial capillary network density and cardiac fibrosis were closer to heart failure manifestations. The above outcomes are consistent with our hypothesis, demonstrating that AS-IV can promote myocardial angiogenesis and thus improve heart failure through the HSF1/VEGF pathway. Previous studies have shown that phosphorylation of HSF1 primarily enhances its activity without affecting HSP70 binding [38], while HSP70 can bind and stabilize VEGF mRNA [39]. These findings suggest that phosphorylation of HSF1 may have limited impact on downstream HSP70/VEGF pathways. However, the influence of HSF1 phosphorylation cannot be completely ruled out, and we plan to investigate the effects of HSF1 phosphorylation sites on heart failure in future studies. In addition, understanding the specific cellular localization of HSF1 in the heart is crucial for comprehensive mechanistic insights, and this aspect will be considered in future research endeavors.

In previous studies, we showed that heightened HSF1 expression enhances proliferation and tube formation in cardiac microvascular endothelial cells, while its depletion has the opposite effect, linked closely to HSF1's regulation of VEGF [30].Angiogenesis

predominantly entails the emergence of new blood vessels through sprouting from the existing vascular network. This process encompasses the degradation of the vascular basement membrane along with the proliferation and movement of endothelial cells. Additionally, it includes the creation of the lumen and the establishment of the vascular system [40]. Angiogenesis of the myocardium helps provide blood flow to ischemic cardiac tissues, effectively reducing cardiac dysfunction. Unlike physiological myocardial hypertrophy, characterized by a significant increase in the number of myocardial microvessels, pathological myocardial hypertrophy is associated with a decrease in microvessel density [41]. In the state of pathological myocardial hypertrophy, myocardial hypoxia promotes myocardial tissue angiogenesis by inducing a reflexive increase in the secretion of VEGF-based angiogenic factors. Consequently, this process coordinates the movement, growth, endurance, and ability of blood vessel lining cells [42,43]. However, when subjected to extended pressure overload, this adaptive angiogenic reaction is suppressed, causing a further decrease in microvessel density and ultimately resulting in significant vascular and cardiac dysfunction. This phenomenon is evident in the cardiac tissues of individuals diagnosed with conditions such as dilated cardiomyopathy, ischemic cardiomyopathy, or inflammatory cardiomyopathy [44],and is thought to play a fundamental role in the development of myocardial hypertrophy leading to decompensated heart failure [41,45]. Drawing from these experiments and clinical observations, it is our conviction that fostering angiogenesis holds great promise as a novel therapeutic avenue in the fight against heart failure. AS-IV, in particular, exhibits remarkable potential in this regard.

AS-IV has been found to promote angiogenesis through PTEN/PI3K/AKT, JAK/STAT3, and ERK1/2 pathways [32,46,47],but similar studies involving heart failure models were all post-infarction heart failure or only at the ex vivo level, and heart failure in TAC models was understudied, and AS-IV has not been reported to be associated with the heat shock protein pathway in existing studies.We innovatively discovered that HSF1 is a new target of AS-IV through network pharmacology and molecular docking, and further validated it in pressure overload-induced heart failure model, and found that AS-IV was also effective in pressure overload-induced heart failure, but its pathway of action differed from that of other disease models, which provided a new theoretical basis for the treatment of AS-IV in heart failure, and our results also side by side illustrated the multi-targeting advantages of Chinese medicine.

Our study identified a new target and pathway of action of AS-IV for the treatment of pressure overload-induced heart failure. Although network pharmacology predicts that binding of AS-IV with HSF1 is likely to occur, the specific mechanism of action remains to be further investigated, which is an important step in the study of the pharmacological effects of Chinese medicinal monomers and one of the directions for our future research.

5. Conclusion

Our experimental results showed that AS-IV could promote VEGF expression and angiogenesis by up-regulating HSF1 and then positively regulating the HSF1/VEGF signaling pathway, increase myocardial capillary density and reduce myocardial fibrosis in pressure-overloaded mice, and then improve cardiac function(Fig. 6). In the realm of traditional Chinese medicine, we revealed novel therapeutic targets of AS-IV for cardiac ailments, potentially offering a fresh theoretical foundation for heart failure management.

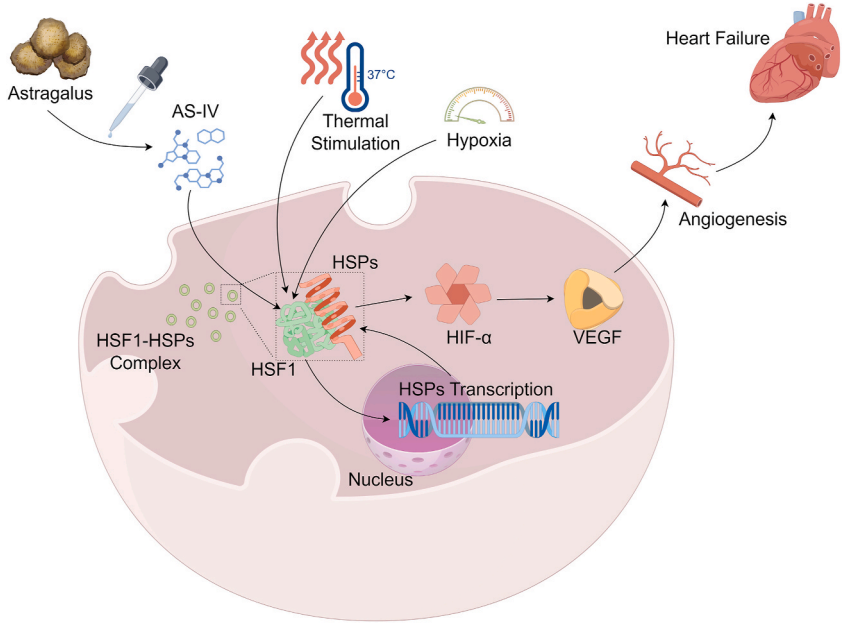

Fig. 6. AS-IV ameliorates pressure overload-induced heart failure by enhancing angiogenesis through HSF1/VEGF pathway (Draw by figdraw, ID: OPWUS242a8).

Ethics statement

Approval for the animal study was granted by the Animal Care Committee and Animal Ethics Committee at the Tongji University (TJBB003223101). The work described has been carried out in accordance with either the U.K. Animals (Scientific Procedures) Act, 1986 and associated guidelines, the European Communities Council Directive 2010/63/EU or the National Institutes of Health – Office of Laboratory Animal Welfare policies and laws. All animal studies must comply with the ARRIVE guidelines.

Data availability statement

The datasets in the study are available from corresponding author on reasonable request.

Funding

This work was supported by the National Natural Science Foundation of China (Grant Nos.82104632 and 82070416).

CRediT authorship contribution statement

Peizhao Du: Writing – review & editing, Writing – original draft, Funding acquisition, Conceptualization. **Linghao Xu:** Writing – review & editing, Writing – original draft, Software, Methodology, Conceptualization. **Yuanqi Wang:** Writing – review & editing, Validation, Formal analysis. **Tiantian Jiao:** Writing – review & editing, Validation, Data curation. **Jing Cheng:** Writing – review & editing, Validation, Data curation. **Chunsheng Zhang:** Writing – review & editing, Formal analysis, Data curation. **Md Sakibur Rahman Tapu:** Writing – review & editing, Formal analysis. **Jian Dai:** Writing – review & editing, Supervision, Conceptualization. **Jiming Li:** Writing – review & editing, Supervision, Funding acquisition, Conceptualization.

Declaration of competing interest

The authors declare that they have no known competing financial interests or personal relationships that could have appeared to influence the work reported in this paper.

Acknowledgements

Not applicable.

Appendix A. Supplementary data

Supplementary data to this article can be found online at https://doi.org/10.1016/j.heliyon.2024.e37019.

References

[1] J.J. McMurray, M.A. Pfeffer, Heart failure, Lancet 365 (9474) (2005) 1877–1889.
[2] P.A. Heidenreich, B. Bozkurt, D. Aguilar, et al., 2022 AHA/ACC/HFSA guideline for the management of heart failure: a report of the American College of Cardiology/American heart association joint committee on clinical practice guidelines, Circulation 145 (18) (2022) e895–e1032.
[3] T.A. McDonagh, M. Metra, M. Adamo, et al., 2023 Focused Update of the 2021 ESC Guidelines for the diagnosis and treatment of acute and chronic heart failure, Eur. Heart J. 44 (37) (2023) 3627–3639.
[4] A. Banerjee, L. Pasea, S.C. Chung, et al., A population-based study of 92 clinically recognized risk factors for heart failure: co-occurrence, prognosis and preventive potential, Eur. J. Heart Fail. 24 (3) (2022) 466–480.
[5] S.J. Greene, J. Bauersachs, J.J. Brugts, et al., Worsening heart failure: nomenclature, epidemiology, and future directions: JACC review topic of the week, J. Am. Coll. Cardiol. 81 (4) (2023) 413–424.
[6] M. Li, B. Han, H. Zhao, et al., Biological active ingredients of Astragali Radix and its mechanisms in treating cardiovascular and cerebrovascular diseases, Phytomedicine 98 (2022) 153918.
[7] M. Monschein, K. Ardjomand-Woelkart, J. Rieder, et al., Accelerated sample preparation and formation of astragaloside IV in Astragali Radix, Pharm. Biol. (2013). Published online October 30.
[8] C. Yang, Q. Pan, K. Ji, et al., Review on the protective mechanism of astragaloside IV against cardiovascular diseases, Front. Pharmacol. 14 (2023) 1187910.
[9] H. Huang, S. Lai, Q. Wan, et al., Astragaloside IV protects cardiomyocytes from anoxia/reoxygenation injury by upregulating the expression of Hes1 protein, Can. J. Physiol. Pharmacol. 94 (5) (2016) 542–553.
[10] Y. Liang, B. Chen, D. Liang, et al., Pharmacological effects of astragaloside IV: a review, Molecules 28 (16) (2023) 6118.
[11] S. Takeda, S. Mochizuki, H.K. Saini, et al., Modification of alterations in cardiac function and sarcoplasmic reticulum by vanadate in ischemic-reperfused rat hearts, J. Appl. Physiol. 99 (3) (2005) 999–1005 (1985).
[12] Y. Ji, T. Wang, X. Zhang, et al., Astragalosides increase the cardiac diastolic function and regulate the "Calcium sensing receptor-protein kinase C-protein phosphatase 1" pathway in rats with heart failure, Biomed. Pharmacother. 103 (2018) 838–843.
[13] H. Shi, P. Zhou, G. Gao, et al., Astragaloside IV prevents acute myocardial infarction by inhibiting the TLR4/MyD88/NF-κB signaling pathway, J. Food Biochem. 45 (7) (2021) e13757.
[14] Z.H. Liu, H.B. Liu, J. Wang, Astragaloside IV protects against the pathological cardiac hypertrophy in mice, Biomed. Pharmacother. 97 (2018) 1468–1478.

[15] M. Lu, H. Wang, J. Wang, et al., Astragaloside IV protects against cardiac hypertrophy via inhibiting the Ca2+/CaN signaling pathway, Planta Med. 80 (1) (2014) 63–69.
[16] J. Yang, H.X. Wang, Y.J. Zhang, et al., Astragaloside IV attenuates inflammatory cytokines by inhibiting TLR4/NF-κB signaling pathway in isoproterenol-induced myocardial hypertrophy, J. Ethnopharmacol. 150 (3) (2013) 1062–1070.
[17] X.Z. Li, Y.Z. Ding, H.F. Wu, et al., Astragaloside IV prevents cardiac remodeling in the apolipoprotein E-deficient mice by regulating cardiac homeostasis and oxidative stress, Cell. Physiol. Biochem. 44 (6) (2017) 2422–2438.
[18] Y. Ma, W. Li, Y. Yin, et al., AST IV inhibits H_2O_2-induced human umbilical vein endothelial cell apoptosis by suppressing Nox4 expression through the TGF-β1/Smad2 pathway, Int. J. Mol. Med. 35 (6) (2015) 1667–1674.
[19] R. Gomez-Pastor, E.T. Burchfiel, D.J. Thiele, Regulation of heat shock transcription factors and their roles in physiology and disease, Nat. Rev. Mol. Cell Biol. 19 (1) (2018) 4–19.
[20] Y. Zou, J. Li, H. Ma, et al., Heat shock transcription factor 1 protects heart after pressure overload through promoting myocardial angiogenesis in male mice, J. Mol. Cell. Cardiol. 51 (5) (2011) 821–829.
[21] S. Kim, J. Chen, T. Cheng, et al., PubChem 2023 update, Nucleic Acids Res. 51 (D1) (2023) D1373–D1380.
[22] A. Daina, O. Michielin, V. Zoete, SwissTargetPrediction: updated data and new features for efficient prediction of protein targets of small molecules, Nucleic Acids Res. 47 (W1) (2019) W357–W364.
[23] G. Stelzer, N. Rosen, I. Plaschkes, et al., The GeneCards suite: from gene data mining to disease genome sequence analyses, Current protocols in bioinformatics 54 (1) (2016) 1–30.
[24] D. Szklarczyk, A. Santos, C. Von Mering, et al., Stitch 5: augmenting protein–chemical interaction networks with tissue and affinity data, Nucleic Acids Res. 44 (D1) (2016) D380–D384.
[25] P. Shannon, A. Markiel, O. Ozier, et al., Cytoscape: a software environment for integrated models of biomolecular interaction networks, Genome Res. 13 (11) (2003) 2498–2504.
[26] Y. Zhou, B. Zhou, L. Pache, et al., Metascape provides a biologist-oriented resource for the analysis of systems-level datasets, Nat. Commun. 10 (1) (2019) 1523.
[27] D. Tang, M. Chen, X. Huang, et al., SRplot: a free online platform for data visualization and graphing, PLoS One 18 (11) (2023) e0294236.
[28] L. Schrodinger, The PyMOL Molecular Graphics system[J], vol. 1, Version, 2015, p. 8.
[29] M.F. Sanner, Python: a programming language for software integration and development, J. Mol. Graph. Model. 17 (1) (1999) 57–61.
[30] P. Du, F. Dai, Y. Chang, et al., Role of miR-199b-5p in regulating angiogenesis in mouse myocardial microvascular endothelial cells through HSF1/VEGF pathway, Environ. Toxicol. Pharmacol. 47 (2016) 142–148.
[31] E. Ji, T. Jiao, Y. Shen, et al., Molecular mechanism of HSF1-upregulated ALDH2 by PKC in ameliorating pressure overload-induced heart failure in mice, BioMed Res. Int. 2020 (2020) 3481623.
[32] S. Cheng, X. Zhang, Q. Feng, et al., Astragaloside IV exerts angiogenesis and cardioprotection after myocardial infarction via regulating PTEN/PI3K/Akt signaling pathway, Life Sci. 227 (2019) 82–93.
[33] J.L. Martindale, N.J. Holbrook, Cellular response to oxidative stress: signaling for suicide and survival, J. Cell. Physiol. 192 (1) (2002) 1–15.
[34] J. Zou, Y. Guo, T. Guettouche, et al., Repression of heat shock transcription factor HSF1 activation by HSP90 (HSP90 complex) that forms a stress-sensitive complex with HSF1, Cell 94 (4) (1998) 471–480.
[35] P. Du, Y. Chang, F. Dai, et al., Role of heat shock transcription factor 1(HSF1)-upregulated macrophage in ameliorating pressure overload-induced heart failure in mice, Gene 667 (2018) 10–17.
[36] L. Pinzi, G. Rastelli, Molecular docking: shifting paradigms in drug discovery, Int. J. Mol. Sci. 20 (18) (2019) 4331.
[37] X. Li, X. Xu, J. Wang, et al., A system-level investigation into the mechanisms of Chinese Traditional Medicine: compound Danshen Formula for cardiovascular disease treatment, PLoS One 7 (9) (2012) e43918.
[38] X. Zheng, J. Krakowiak, N. Patel, A. Beyzavi, J. Ezike, A.S. Khalil, et al., Dynamic control of Hsf1 during heat shock by a chaperone switch and phosphorylation, Elife 5 (2016) e18638, https://doi.org/10.7554/eLife.18638 [pii].
[39] A. Kishor, B. Tandukar, Y.V. Ly, E.A. Toth, Y. Suarez, G. Brewer, et al., Hsp70 is a novel posttranscriptional regulator of gene expression that binds and stabilizes selected mRNAs containing AU-rich elements, Mol. Cell Biol. 33 (1) (2013) 71–84, https://doi.org/10.1128/MCB.01275-12.
[40] G. Eelen, L. Treps, X. Li, et al., Basic and therapeutic aspects of angiogenesis updated, Circ. Res. 127 (2) (2020) 310–329.
[41] T. Oka, H. Akazawa, A.T. Naito, et al., Angiogenesis and cardiac hypertrophy: maintenance of cardiac function and causative roles in heart failure, Circ. Res. 114 (3) (2014) 565–571.
[42] G.L. Semenza, Hypoxia-inducible factors in physiology and medicine, Cell 148 (3) (2012) 399–408.
[43] C.W. Pugh, P.J. Ratcliffe, Regulation of angiogenesis by hypoxia: role of the HIF system, Nat Med 9 (6) (2003) 677–684.
[44] R. Karch, F. Neumann, R. Ullrich, et al., The spatial pattern of coronary capillaries in patients with dilated, ischemic, or inflammatory cardiomyopathy, Cardiovasc. Pathol. 14 (3) (2005) 135–144.
[45] Y.K. Tham, B.C. Bernardo, J.Y. Ooi, et al., Pathophysiology of cardiac hypertrophy and heart failure: signaling pathways and novel therapeutic targets, Arch. Toxicol. 89 (9) (2015) 1401–1438.
[46] Y.B. Sui, Y. Wang, L. Liu, et al., Astragaloside IV alleviates heart failure by promoting angiogenesis through the JAK-STAT3 pathway, Pharm. Biol. 57 (1) (2019) 48–54.
[47] S.G. Wang, Y. Xu, J.D. Chen, et al., Astragaloside IV stimulates angiogenesis and increases nitric oxide accumulation via JAK2/STAT3 and ERK1/2 pathway, Molecules 18 (10) (2013) 12809–12819.